GeoHealth

RESEARCH ARTICLE
10.1029/2021GH000429

Key Points:

- Increases in deforestation among states analyzed in the Brazilian Legal Amazon since 2012 increased the dry season fire count by 39% in 2019
- This increase in fire resulted in 3,400 (3,300–3,550) additional deaths in 2019 due to increased exposure to particulate air pollution
- Our analysis demonstrates the strong benefits of reduced deforestation on air quality and public health across the Amazon

Supporting Information:

Supporting Information may be found in the online version of this article.

Correspondence to:

E. W. Butt,
e.butt@leeds.ac.uk

Citation:

Butt, E. W., Conibear, L., Knote, C., & Spracklen, D. V. (2021). Large air quality and public health impacts due to Amazonian deforestation fires in 2019. *GeoHealth*, *5*, e2021GH000429. https://doi.org/10.1029/2021GH000429

Received 25 MAR 2021
Accepted 14 JUN 2021

Author Contributions:

Conceptualization: Edward W. Butt, Dominick V. Spracklen
Formal analysis: Edward W. Butt
Methodology: Edward W. Butt, Dominick V. Spracklen
Software: Christoph Knote
Visualization: Edward W. Butt
Writing – original draft: Edward W. Butt, Dominick V. Spracklen
Writing – review & editing: Edward W. Butt, Luke Conibear, Christoph Knote, Dominick V. Spracklen

Large Air Quality and Public Health Impacts due to Amazonian Deforestation Fires in 2019

Edward W. Butt[1], Luke Conibear[1], Christoph Knote[2], and Dominick V. Spracklen[1]

[1]School of Earth and Environment, University of Leeds, Leeds, UK, [2]Medical Faculty, University of Augsburg, Augsburg, Germany

Abstract Air pollution from Amazon fires has adverse impacts on human health. The number of fires in the Amazon has increased in recent years, but whether this increase was driven by deforestation or climate has not been assessed. We analyzed relationships between fire, deforestation, and climate for the period 2003 to 2019 among selected states across the Brazilian Legal Amazon (BLA). A statistical model including deforestation, precipitation and temperature explained ~80% of the variability in dry season fire count across states when totaled across the BLA, with positive relationships between fire count and deforestation. We estimate that the increase in deforestation since 2012 increased the dry season fire count in 2019 by 39%. Using a regional chemistry-climate model combined with exposure-response associations, we estimate this increase in fire resulted in 3,400 (95UI: 3,300–3,550) additional deaths in 2019 due to increased exposure to particulate air pollution. If deforestation in 2019 had increased to the maximum recorded during 2003–2019, the number of active fire counts would have increased by an additional factor of 2 resulting in 7,900 (95UI: 7,600–8,200) additional premature deaths. Our analysis demonstrates the strong benefits of reduced deforestation on air quality and public health across the Amazon.

Plain Language Summary Exposure to air pollution created from fires in the Amazon fires has detrimental impacts on human health. The number of active fires across the Brazilian Legal Amazon (BLA) has increased in recent years, but the reason for this increase has not been fully assessed to-date. Using a statistical model, we found that increases in BLA deforestation rate since 2012 increased dry season fire count in 2019 by 39%. Using a regional chemistry-climate model, we estimated that this increase in fire count resulted in 3,400 (95UI: 3,300–3,550) additional human deaths in 2019 due to increased population exposure to fine particulate matter air pollution. We also found that if deforestation in 2019 had increased to the maximum recorded during 2003–2019, the number of active fires would have increased by an additional factor of 2 resulting in 7,900 (95UI: 7,600–8,200) additional deaths. The findings of our analysis demonstrate the strong benefits of reduced deforestation on air quality and public health across the Amazon region.

1. Introduction

Recent increases in deforestation and fire in the Brazilian Legal Amazon (BLA) have caused widespread concern and considerable media attention (Barlow et al., 2019). Deforestation results in biodiversity loss (Barlow et al., 2016) and large greenhouse gas emissions (Anderson et al., 2015). Fires also emit a range of air pollutants (Wiedinmyer et al., 2011), degrading air quality, and impacting public health (Reddington et al., 2015). However, the impacts of recent increases in deforestation and fire across the BLA on air quality have not been assessed. Here we combine satellite data on deforestation and fire with a regional air quality model to make a first estimate of how increased deforestation and fire across the BLA have degraded air quality.

Fires are the dominant source of fine particulate matter ($PM_{2.5}$, particulate matter with an aerodynamic median diameter less than 2.5 μm) over the Amazon (Artaxo et al., 2013; Brito et al., 2014; Martin et al., 2010; Mishra et al., 2015; Reddington et al., 2016, 2019). Exposure to $PM_{2.5}$ is a leading global and regional risk factor for public health (Cohen et al., 2017). Exposure to fire-derived $PM_{2.5}$ has been shown to have adverse impacts on public health (Butt et al., 2020; Johnston et al., 2012; Lelieveld et al., 2015; Nawaz & Henze, 2020; Reddington et al., 2015; Sant'Anna & Rocha, 2020). If Amazon fires could be prevented, it is estimated that the reduced exposure to $PM_{2.5}$ would prevent 7,000 to 17,000 premature deaths annually (Butt et al., 2020;

Johnston et al., 2012; Reddington et al., 2015). Greater understanding of the connections between land-use change, fire and air quality is therefore crucial to improving public health across the region (Reddington et al., 2015).

Amazonian fires result from a complex interplay between climate, vegetation, and people (Cochrane, 2003). Most fires occur in the dry season between July and November, peaking in September for the southern parts of the Basin (Chen et al., 2013; Martin et al., 2010). Droughts are strongly correlated with greater fire number (Aragão et al., 2007, 2018), increasing fire risk through reduced ground water and surface humidity (Ray et al., 2005). Statistical models have been developed that predict fire activity using sea surface temperature anomalies in the tropical Atlantic and Pacific (Chen et al., 2011; Fernandes et al., 2011; Lima et al., 2018). However, such predictions based solely on climate miss the important role of people in altering fire across the Amazon.

People make extensive use of fires across the Amazon to create and maintain agricultural land (Cochrane, 2003; Morton et al., 2008). Forests are cut in the wet season and the vegetation is left to dry before fires are lit to clear vegetation. The number of fires is therefore greater in years with more deforestation (Aragão et al., 2008, 2018; Chen et al., 2013; Reddington et al., 2015). Fires can spread from recently cleared areas into surrounding forests. Deforestation and forest degradation result in a fragmented forest landscape that is more prone to fire (Alencar et al., 2015; Cano-Crespo et al., 2015). Understorey fires can cause large-scale tree mortality (Barlow et al., 2003; Brando et al., 2014), degrading the forest and impacting microclimate and leading to further susceptibility to fire (Cochrane et al., 1999). In recent years, extreme droughts have resulted in dry leaf litter (Ray et al., 2005) even in primary forest and large areas have burned (Withey et al., 2018).

Deforestation also alters regional climate, increasing local temperatures (Baker & Spracklen, 2019) and reducing regional rainfall (Spracklen & Garcia-Carreras, 2015; Spracklen et al., 2012; Zemp et al., 2017). Smoke from fires further reduces rainfall through interactions with clouds and radiation (Archer-Nicholls et al., 2016; Kolusu et al., 2015; Liu et al., 2020). Positive feedbacks between deforestation, drought, fire, and smoke exacerbate the potential for tipping points in Amazonian climate (Lovejoy & Nobre, 2018; Nepstad et al., 2008).

Large-scale deforestation of the Amazon started in the 1970s, and ~15% of the original forested area had been deforested by 2010 (Aragão et al., 2014). Very few fires occurred in the Amazon before the onset of deforestation and fire emissions increased in line with deforestation (van Marle et al., 2017). Rates of deforestation in the BLA were high through the late-1980s and early-2000s, averaging 19,000 km^2 per year between 1988 and 2005 (Assis et al., 2019). Well-documented reductions in deforestation occurred after 2004 (Aragão et al., 2014; Hansen et al., 2013) with deforestation rates declining by 75% to a minimum of 4,571 km^2 in 2012 (Assis et al., 2019). Reductions in deforestation across the Amazon between 2001 and 2012 have been linked to reduced fire emissions and improved air quality preventing 400 to 1,700 premature deaths annually (Reddington et al., 2015). However, more frequent droughts in recent years (Marengo & Espinoza, 2016) and increased forest degradation may have counteracted some of the reduction in fire activity due to declines in deforestation (Aragão et al., 2018).

Since 2012, rates of deforestation across the BLA have increased by a factor of 2, with 10,129 km^2 deforested in 2019 (Assis et al., 2019; Barlow et al., 2019). The impact of this increased deforestation on the amount of fire is still uncertain (Aragão et al., 2018; Libonati et al., 2021; van Marle et al., 2017) and the impacts on air quality have not yet been fully assessed. To estimate the impact of increased deforestation on fire, we developed a model to predict dry season active fire count based on climate and deforestation. We used this model to predict how the number of fires in 2019 would change under different deforestation scenarios. Finally, we used a climate-chemistry model and exposure-response associations to simulate the air quality impacts under these different deforestation scenarios.

2. Method

2.1. Satellite Data

2.1.1. Aerosol Optical Depth Measurements

We used spectral columnar aerosol optical depth (AOD) obtained from Moderate resolution Imaging Spectroradiometer (MODIS) on Aqua and Terra satellites. Collection 6.1, level 2, AOD was acquired at 550 nm for the data set "Dark Target Deep Blue Combined" (Levy et al., 2013). Swaths of 10 km (at nadir) were resampled to 0.1° × 0.1° resolution. Data were aggregated to daily means. Because daytime overpass times are different for both Terra (10:30 LT) and Aqua (13:30 LT), we used simulated AOD averaged between both overpass times and evaluated only on days when satellite data were available.

2.1.2. Active Fire Count Data

Active fire count data were taken from Collection 6 Terra and Aqua MODIS fire product (MCD14DL). Our analysis includes all fire types including fires associated with deforestation, pasture maintenance, and agricultural fires and wildfires that spread into surrounding forest. Fire detection is performed using a contextual algorithm that exploits the strong emission of mid-infrared radiation from fires (Giglio et al., 2003, 2006). The MODIS instrument on board Terra and Aqua satellites acquire data continuously providing global coverage every 1–2 days. The terra satellite passes over the equator at ~10:30 a.m. and 10:30 p.m. each day and the Aqua satellite passes over the equator at ~1:30 p.m. and 1:30 a.m. MODIS fire count data is available from November 2000 (for Terra) and from July 2002 (for Aqua) to the present. We obtained data for the period 2003 to 2019 through the MODIS Fire Archive Download Tool.

2.1.3. Deforestation Data

State-level deforestation rates from the Brazilian government's satellite monitoring program known as Program to Calculate Deforestation in the Amazon (PRODES) and the near real-time deforestation detection were taken from the National Institute for Space Research (INPE) TerraBrasilis platform (Assis et al., 2019). PRODES captures new, clear-cut deforestation of primary forest in areas larger than 6.25 hectares, such that once deforestation occurs; the area is excluded from future monitoring. PRODES monitoring runs over a 12-month period from August 1 to July 31, such that PRODES data for 2019 reference year includes deforestation that occurred between August 1, 2018 and July 31, 2019. This time period, which is in the middle of the dry season, allows for better image collection since the forest is less likely to be covered by clouds, as well as coinciding with typical clearing cycles in the region.

2.1.4. Precipitation Data

We used the Climate Hazards Group InfraRed Precipitation with Stations (CHIRPS) monthly gridded satellite precipitation data set. The CHIRPS data set is a blended rainfall product combining a pentadal precipitation climatology, satellite observations, atmospheric model simulated rainfall fields, and in situ observations from gauge stations. Quasi-global gridded products are available from 1981 to near-present at 0.05° spatial resolution (~5.3 km) (Funk et al., 2014).

2.1.5. Land Surface Temperature

We used monthly mean land surface temperature (LST) data from MODIS Terra Collection 006. The data set was provided by the Integrated Climate Data Centre (Wan et al., 2015). LST was obtained using a split window technique from radiances obtained under clear-sky conditions. LST was calculated for each day first for single MODIS overpasses, then for tiles with 1,000 m resolution (product MOD11A1) and finally to a 0.05° grid resolution. To produce the final data product, other MODIS products were used: vertical temperature and water vapor profiles, the MODIS cloud mask, the land cover distribution, and the snow cover. We use Terra with 10:30 a.m. overpass time to enhance the number of clear-sky retrievals compared to Aqua (1.30 p.m. overpass).

Table 1
Correlation Between Active Dry Season Fire Count, and Individual Features of Deforestation Rate, LST, Precipitation (P, Wet Season and Dry Season), AOD, and Fire Organic Carbon Emissions at the State Level Across the BLA During 2003 to 2019

State[a]	Deforestation	LST	Wet season P	Dry season P	AOD	Fire emissions	Fire count (per Mha)	Deforestation rate (km^2 per Mha)
Acre	0.47	0.07	−0.37	−0.18	0.37	0.8	463	24
Amazonas	0.25	0.21	−0.2	−0.42	0.3	0.85	92	5
Maranhão	0.11	0.6	−0.37	−0.53	0.25	0.91	1,003	16
Mato Grosso	0.77	−0.24	−0.31	−0.36	0.8	0.9	823	35
Para	0.62	0.11	−0.22	−0.36	0.9	0.84	567	33
Rondônia	0.83	−0.38	−0.35	−0.2	0.85	0.9	1,112	64
Tocantins	−0.06	0.62	−0.66	−0.55	0.7	0.9	924	3

Note. Mean number of dry season fires and mean deforestation rates are also shown.

Abbreviations: AOD, aerosol optical depth; BLA, Brazilian Legal Amazon; LST, land surface temperature.

[a]Acre dry (wet) season: July–October (November–May); Amazonas dry (wet) season: July–November (November–May); Maranhão dry (wet) season: June–December (December–April); Mato Grosso dry (wet) season: June–October (November–April); Para dry (wet) season: July–December (December–May); Rondônia dry (wet) season: July–October (November–May); Tocantins dry (wet) season: July–October (November–April).

2.2. Models

2.2.1. General Linear Model

Fire risk in the Amazon is strongly influenced by climate (Lima et al., 2018). The seasonal cycle of fire count (Figure S1) closely resembles precipitation and LST (Figures S2 and S3), with a greater number of fires during dry season periods. We analyzed fires at the state level across the BLA. We include all states in the BLA except the northern states of Roraima and Amapa that have distinctly different dry seasons.

We used a general linear modeling (GLM) framework to predict dry season active fire count at the state level. We included precipitation and LST as predictor variables, as used in previous studies (e.g., Lima et al., 2018). To explore the role of deforestation, we also included annual deforestation at the state level as a predictor. We modeled the number of dry season fires at the state level (Y_t, fires per Mha) as a function of independent variables indexed by time *t:*

$$Y_t = \alpha 0 + \alpha 1 \cdot \mathrm{WP}_t + \alpha 2 \cdot \mathrm{DP}_t + \alpha 3 \cdot \mathrm{DT}_t + \alpha 4 \cdot D_t, \quad (1)$$

where WP_t, DP_t, DT_t, and D_t are preceding wet season precipitation, dry season precipitation, dry season LST, and annual deforestation rate (August–July) within a given reference year, respectively. We define dry season and wet season at the state level as shown in Table 1, based on seasonal cycle of precipitation and LST (Figures S2 and S3). Dry season LST was calculated as the average of daily data across the state. Dry and wet season precipitation were calculated as an average of the monthly data across the state. We treat deforestation and climate variables as independent predictor variables although note there may be a two-way relationship between the deforestation rate and drought, which will be partially represented within PRODES deforestation data. As a measure of GLM accuracy, we use the adjusted r^2 as an unbiased estimate of the fraction of variance explained, taking into account the sample size and number of predictor variables.

2.2.2. Weather Research and Forecasting Online-Coupled Chemistry Model

We used the Weather Research and Forecasting online-coupled Chemistry (WRF-Chem) model version 3.7.1 (Grell et al., 2005). An identical model setup to that described here was evaluated in detail against surface, airborne, and satellite observations (Butt et al., 2020). The model domain covers most of South America (Figure S4) with a horizontal resolution of 30 km, extending vertically from the surface to 10 hPa. Details of model setup are shown in Table S1. Gas-phase chemistry is calculated using the extended Model for Ozone and Related Chemical Tracers, version 4 (MOZART-4) (Emmons et al., 2010; Knote et al., 2014). Aerosol chemistry and microphysics is simulated using an updated Model for Simulating Aerosol Interaction and

Chemistry (MOSAIC) with aqueous chemistry and four sectional discrete aerosol size bins: 0.039–0.156 μm, 0.156–0.625 μm, 0.625–2.5 μm, 2.5–10 μm (Hodzic & Knote, 2014; Zaveri et al., 2008). An updated volatility basis set mechanism was also included for secondary organic aerosol (SOA) formation (Knote et al., 2015). Microphysics is simulated using the Morrison 2-moment scheme (Morrison et al., 2009) and the Grell 3-D parameterization is used for simulating convection (Grell & Dévényi, 2002). Initial and boundary chemistry and aerosol conditions were taken from 6-hourly simulation data from the MOZART-4/Goddard Earth Observing System Model version 5 (National Center for Atmospheric Research, 2019). Initial and boundary meteorological conditions were taken from the European Centre for Medium-Range Weather Forecasts (ECMWF) ERA5 global reanalysis (ECMWF, 2017). During model simulations, we nudged the meteorological components, horizontal and vertical wind, potential temperature, and water vapor mixing ratio, to ECMWF reanalysis in all model levels above the planetary boundary layer (BL) over 6 h.

2.2.3. WRF-Chem Nonfire Emissions

Anthropogenic emissions were taken from the Emission Database for Global Atmospheric Research with Task Force on Hemispheric Transport of Air Pollution version 2.2 for the year 2010 at 0.1° × 0.1° horizontal resolution (Janssens-Maenhout et al., 2015). A diurnal cycle was applied to anthropogenic emissions (Olivier et al., 2003). Biogenic volatile organic compound and dust emissions were both calculated online by the Model of Emissions of Gases and Aerosol from Nature (Guenther et al., 2006) and through Goddard Global Ozone Chemistry Aerosol Radiation and Transport with Air Force Weather Agency modification (Chin et al., 2000), respectively.

2.2.4. WRF-Chem Fire Emissions

We used fire emissions in 2019 from the Fire Inventory from NCAR (FINN) (Wiedinmyer et al., 2011). Daily emissions are estimated on a 1 km^2 grid based on the location and timing of active fires taken from MODIS Fire and Thermal Anomalies Product (Giglio et al., 2003). Each fire count is assigned a burned area: 0.75 km^2 for grassland and savannah and 1 km^2 for other land in line with biomass fuels associated with MODIS Land Cover Type and Vegetation Continuous Fields.

FINN fire emission are emitted in WRF-Chem using a diurnal cycle that peaks in the early afternoon (local-time) based on Giglio (2007) and are injected evenly throughout the BL, as supported by fire emission plume heights over the Amazon (Marenco et al., 2016).

At the time of this analysis, the current scientific release version of FINN (v1.5) did not include fire emissions for 2019. Instead, we used the FINN near-real-time (NRT) product v1 for 2019. We scaled FINN NRT emissions in 2019 by the ratio of emissions in FINN v1.5 to FINN NRT v1 in 2018 (Figure S5). A comparison of WRF-Chem simulated dry season AOD using the original FINN NRT v1 and scaled 2019 emissions to MODIS AOD showed a better match for the scaled emissions (Figure S6), with a good comparison across the BLA (mean bias between −0.1 to 0.1; see Figure S7c), and consistent with others studies (e.g., Archer-Nicholls et al., 2015, 2016) (Butt et al., 2020). Table S2 shows annual and dry season OC and BC emissions summed over the BLA. The dry season (1 July–31 October) contributes 70%–80% of annual emissions of OC and BC. In 2019, dry season OC (BC) emissions were 18% (17%) lower than the 2003–2018 average, and 35% (35%) lower than the 2003–2012 average (high deforestation). However, dry season OC (BC) emissions in 2019 were 29% (28%) higher than the 2013–2018 average (initially low deforestation). Compared to 2018, OC (BC) emissions were 29% (29%) higher in 2019. Comparing emissions in 2019 to the 2003–2012 average, displays a distinct dipole across the BLA, which can be explained by a northward shift in deforestation and associated fires in recent years (Figure S8). In contrast, emissions in 2019 compared to the 2013–2018 average (Figure S8c) show an increase across the BLA largely due to the higher deforestation in 2019.

2.2.5. WRF-Chem Simulations in 2019

WRF-Chem model simulations were conducted for the year 2019 from April to December, with 1-month spin-up. We conducted four simulations with different fire emissions: (a) Wiedinmyer et al. (2011) (baseline) emissions, (b) no fire emissions in the BLA, (c) fire emissions under a minimum deforestation scenario, (d) fire emissions under a maximum deforestation scenario.

The difference between simulations (a) and (b) was used to quantify the contribution of vegetation fires on regional air quality and its impacts on public health in 2019. The difference between simulations (a) and (c) and (a) and (d) were used to quantify the impact of different deforestation scenarios.

For each state, we defined a maximum deforestation scenario as the maximum deforestation rate that had occurred between 2003 and 2019, and a minimum deforestation scenario as the minimum deforestation rate that had occurred during this period. We then applied these deforestation rates in the state-level GLMs to predict the fire count under these scenarios ($fires_{scenario}$). Based on the strong relationship between observed fires and emissions (Figure S9), we then used these changes in predicted fires count to calculate emissions at the state level:

$$modified_{emis} = \left(\frac{fires_{scenario}}{fires_{base}}\right) baseline_{emis} \quad (2)$$

where $modified_{emis}$ is calculated emissions scenario, $fires_{base}$ is the GLM baseline predicted fire count at the state level, and $baseline_{emis}$ is the baseline FINN emissions in 2019.

We did not scale state-level fire emissions under deforestation scenarios if maximum or minimum rates of deforestation between 2003 and 2019 were the same as in 2019 (see Table 1).

2.3. Health Burden Calculation

We used simulated annual mean surface $PM_{2.5}$ concentrations to quantify the health impact due to fires through the disease burden attributable to air pollution exposure. To estimate annual mean $PM_{2.5}$, we assumed simulated concentrations in April and December are representative of January–March, when fire emissions are also low. This assumption is reasonable given the seasonality of observed fire count across states (Figure S1), and simulated $PM_{2.5}$ evaluated in Butt et al. (2020).

Using population attributable fractions of relative risk taken from associational epidemiology, population exposures under different fire scenarios were used to predict associated variations in health burden outcomes. The population attributable fraction (PAF) was estimated as a function of population (P) and the relative risk (RR) of exposure:

$$PAF = P \times \left(RR_{EXP} - 1 / RR_{EXP}\right) \quad (3)$$

RR estimates are taken from the Global Exposure Mortality Model (GEMM), which can be accessed through Burnett et al. (2018). We used the GEMM for nonaccidental mortality (noncommunicable disease, NCD, plus lower respiratory infections, LRI), using parameters including the China cohort, with age-specific modifiers for adults over 25 years of age in 5-year intervals. The GEMM functions have mean, lower, and upper uncertainty intervals. The theoretical minimum-risk exposure level for the GEMM functions is 2.4 $\mu g\ m^{-3}$. The toxicity of $PM_{2.5}$ was treated as homogenous with no differences for source, shape, or chemical composition, due to a lack of associations among epidemiological studies.

The effect of air pollution is known to be significantly different for morbidity and mortality from cardiovascular outcomes (ischemic heart disease, IHD and stroke, and STR) (Cohen et al., 2017), and the relative risks from Equation 3 were adjusted by Equation 4 ($RR_{adjusted}$) when estimating years lived with disability (YLD). The ratio for IHD and STR morbidity were 0.141 and 0.553 from the GBD2016 (Cohen et al., 2017), based on data from three cohort studies (Lipsett et al., 2011; Miller et al., 2007; Puett et al., 2009)

$$RR_{EXP,adjusted} = ratio \times RR_{EXP} - ratio + 1 \quad (4)$$

Premature mortality (MORT), years of life lost (YLL), and years lived with disability (YLD) per health outcome, age bracket, and grid cell were estimated as a function of the PAF and corresponding country-level baseline mortality (I_{MORT}), YLL (I_{YLL}), and YLD (I_{YLD}) taken from GBD2017 (Roth et al., 2018) following Equations 5–7, respectively.

$$MORT = PAF \times I_{MORT} \quad (5)$$

$$YLL = PAF \times I_{YLL} \quad (6)$$

$$YLD = PAF \times I_{YLD} \quad (7)$$

Disability-adjusted life years (DALYs), that is, the total loss of healthy life, was estimated as the total of YLL and YLD:

$$DALYs = YLL + YLD \quad (8)$$

The rates of MORT, YLL, YLD, and DALYs were calculated per 100,000 population. Mean estimates were quantified in addition to upper and lower uncertainty intervals at the 95% confidence level. The United Nations adjusted the population count data set for 2020 at 0.25° × 0.25° resolution was obtained from the Gridded Population of the World, Version 4 (GPWv4) Revision 11 (Center for International Earth Science Information Network—CIESIN—Columbia University, 2018). Population age composition was taken from the GBD2017 for 2015 for early-neonatal (0–6 days), late-neonatal (7–27 days), post-neonatal (8–364 days), 1–4 years, 5–95 years in 5-year intervals, and 95 years plus (Roth et al., 2018). Shapefiles were used to aggregate results at the country and state level (Hijmans, 2012).

The health impacts of $PM_{2.5}$ depend nonlinearly on exposure, with impacts starting to saturate at high $PM_{2.5}$ concentrations (Burnett et al., 2014, 2018). We estimate the health benefits that would arise if fires were prevented, as the health burden from a scenario with fires minus the health burden from a scenario without fires (but including other nonfire PM emission sources). This is described as the "subtraction" method (Conibear et al., 2018; Kodros et al., 2016).

Fires in the BLA exhibit low interannual variability due to widespread and routine human-induced burning (Giglio et al., 2013) that has been occurring since the late 1980s when widespread deforestation began (van Marle et al., 2017). This means that populations in the BLA have been consistently exposed to PM2,5 from fires for more than 30 years, justifying our focus on the impacts of long-term exposure to PM2.5 as applied in previous studies in the Amazon (Butt et al., 2020) and Equatorial Asia (Crippa et al., 2016; Kiely et al., 2020; Koplitz et al., 2016).

3. Results and Discussion

3.1. Prediction of Amazon Fires

Figure 1 shows the relationship between the dry season active fire count, deforestation rate, fire emissions, and AOD across the BLA between 2003 and 2019. Simultaneous peaks in fire count, fire emissions, and AOD occur during drought years (2005, 2007, 2010, and 2015). Declines in fire count, emissions, and AOD follow declines in deforestation during 2001–2014, as reported previously (Reddington et al., 2015). Fire count, emissions, AOD, and deforestation have all increased from 2014 to 2019, confirming previously identified links between fires and deforestation (Aragão et al., 2008, 2018; Barlow et al., 2019; Reddington et al., 2015).

We analyzed relationships between dry season total fire count from all fire types, individually with deforestation rate, precipitation, LST, and AOD at the state level across the BLA (Figure 2 and Table 1). Total fire count tended to be positively related with the deforestation rate, particularly in states with substantial deforestation, such as Rondônia (Pearson's correlation coefficient [r], $r = 0.83$), Mato Grosso ($r = 0.77$), and Para ($r = 0.62$) (Table 1). Analysis of the monthly deforestation rate and fire count shows that deforestation peaks at the end of the wet season, before the dry season peak in fires (Figure S10). This suggests that within a specific year, fires are not the dominant cause of deforestation. In all states, total fire count was negatively related to both wet and dry season precipitation ($r = -0.2$ to -0.7). The link with dry season precipitation suggests an important dry season precipitation control on fires. We note that dry and wet season precipitation are weakly related at the state level (Figure S11), so links between wet season precipitation and fire are distinct from links between dry season precipitation and fire. The relationship with wet season precipitation is therefore suggestive of a legacy effect, possibly through controls on dry season soil water content and

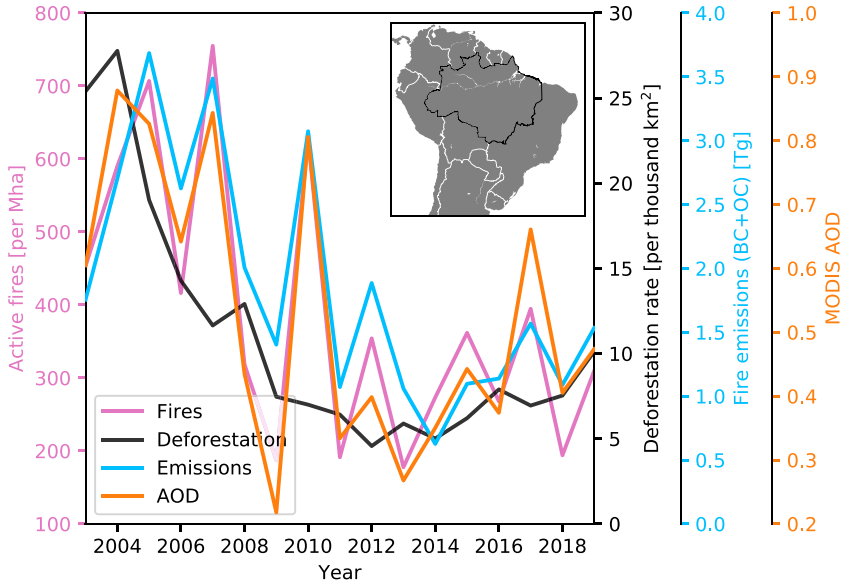

Figure 1. Time-series of dry season (1st July to 31st October) active fire count, annual deforestation rate, fire particulate emissions (black carbon, BC and organic carbon, OC), and aerosol optical depth (AOD) over the Brazilian Legal Amazon (BLA). The insert map image shows the boundary of the BLA (black line) and extent of the Weather Research and Forecasting online-coupled Chemistry model domain.

associated humidity. Relationships between dry season fire and LST were generally positive. States with low deforestation rates, such as Maranhão and Tocantins exhibited stronger correlations between fire and climate (precipitation and LST). The number of fires is positively correlated with fire emissions and AOD, demonstrating the strong control of fire on regional air quality (Table 1).

We developed a GLM for states across the BLA to predict the dry season fire count based on the deforestation rate, wet season rainfall, dry season rainfall, and LST (Table 2). In general, deforestation and LST have a positive effect on fires, while wet and dry season rainfall have a negative effect on fires (Figure 3). The GLM provides a good prediction of fire count, particularly for states with substantial number of fires, such as Maranhão ($r^2 = 0.56$; p value $= 0.007$), Mato Grosso ($r^2 = 0.75$; $p = 0.0002$), Para ($r^2 = 0.53$; $p = 0.01$), and Rondônia ($r^2 = 0.71$; $p = 0.0006$) (Table 2). Crucially, GLM predictions of the fire count in these states is considerably better when the deforestation rate is included as a predictor in addition to climate (Table 2), as has been shown previously (Silvestrini et al., 2011). These states have the biggest impacts on regional air quality, contributing 81% of active fire count and 92% of organic carbon fire emissions across the all the states analyzed in BLA between 2003 and 2019. The GLM is less accurate for states with lower fire count and emissions including Amazonas, Acre, and Tocantins. Summed to the BLA level, our state-level GLMs are able to make good predictions of total dry season fires (Figure 4; $r^2 = 0.8$).

3.2. Fires in 2019 Under High and Low Deforestation Scenarios

We used these GLMs to predict how the recent increase in the rate of deforestation has increased the incidence of active fire count. For each state we identified the minimum annual deforestation rate that had occurred during 2003–2019. We then combined this deforestation rate with the GLM to calculate the number of fires that would have occurred (Table 3). Under this minimum deforestation scenario, we estimate that the number of dry season fires summed across the BLA would have reduced by 28% in 2019, with large reductions in Acre (93%), Amazonas (41%), Para (47%), and Rondônia (50%). This means that the factor of 2 increase in the deforestation rate across the BLA between 2014 and 2019 has increased the fire count across the BLA by 39%.

Despite the recent increase in deforestation across the BLA, the deforestation rate is still lower than the maximum rate experienced in the last few decades (Figure 1). If the deforestation rate in 2019 had returned to these historically high levels, it is likely that the fire count would have been even greater than experienced

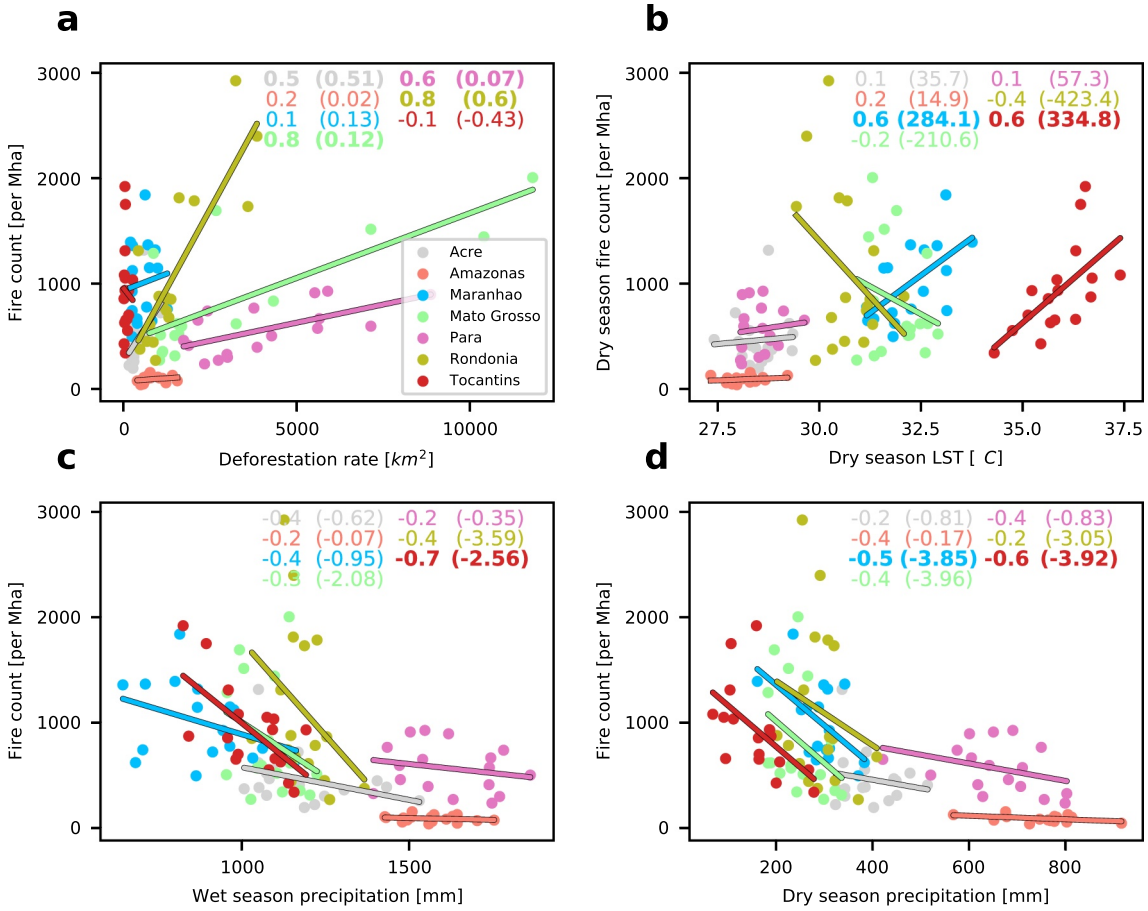

Figure 2. Relationship between dry season active fire count and (a) annual deforestation rate, (b) dry season land surface temperature (LST), (c) wet season precipitation, and (d) dry season precipitation over the states analyzed in Brazilian Legal Amazon (BLA). Pearson's correlation coefficient (r) and slope of best-fit line (in parenthesis) are shown on each panel for each state located with the BLA. Bold values indicate significant relationships ($r > 0.5$).

in 2019. We estimated the amount of fire that would have occurred in 2019 if deforestation had increased to the maximum rate observed during 2003–2019. For each state, we identified the maximum deforestation rate that occurred during 2003–2019 and predicted the change of fire in 2019 under this maximum

Table 2
GLM Predictions of Total Dry Season Fire Count at the State Level

	Including deforestation			Excluding deforestation		
State	r^2	Adjusted r^2	P-value	r^2	Adjusted r^2	P-value
Acre	0.508	0.344	0.0575	0.154	−0.041	0.521
Amazonas	0.335	0.113	0.261	0.229	0.051	0.321
Maranhão	0.667	0.556	0.00686	0.510	0.397	0.022
Mato Grosso	0.815	0.753	0.000236	0.604	0.512	0.006
Para	0.645	0.526	0.00978	0.284	0.119	0.212
Rondônia	0.784	0.712	0.000576	0.704	0.635	0.000964
Tocantins	0.574	0.432	0.0266	0.565	0.465	0.0107

Note. GLMs were run both including and excluding deforestation rate as a predictor variable, but all included climate predictor variables wet and dry season precipitation, and dry season land surface temperature. GLM metrics and estimates reported in the main text of this study are those including deforestation as a predictor variable.
Abbreviation: GLM, general linear modeling.

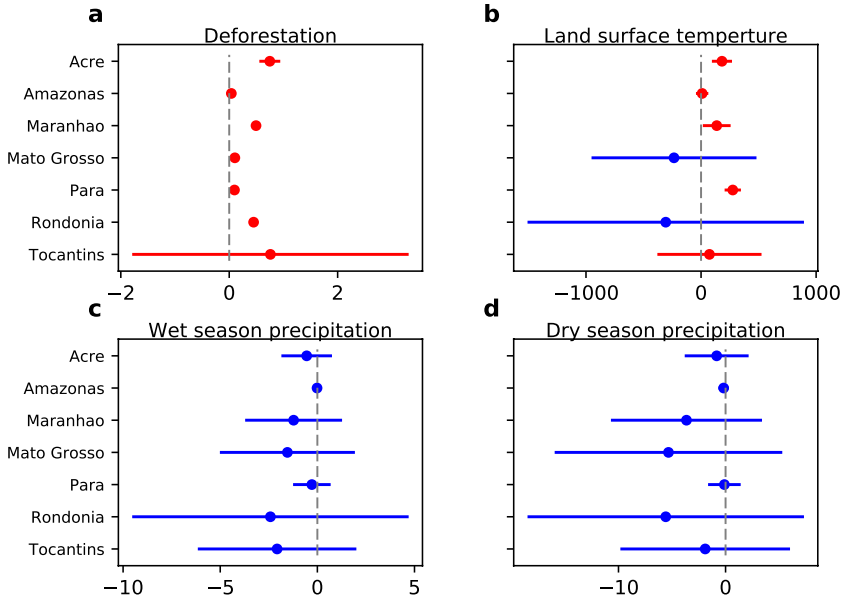

Figure 3. Coefficients (colored dots) and 95% confidence intervals (arrows) from the general linear modeling analysis (a) Deforestation (b) Land surface temperature (LST) (c) Wet season precipitation and (d) Dry season precipitation. Estimates of covariates having a positive (red) and negative (blue) effect on fires are indicated.

deforestation scenario (Table 3). Under this maximum deforestation scenario, the total number of active fires across the BLA would have been a factor of 2 greater than actually experienced in 2019, with particularly large increases in Mato Grosso (137%), Para (112%), and Rondônia (160%).

The highest rates of deforestation were experienced across most of the states in the BLA in the early 2000s (2003–2005). Environmental policies are now quite different. For example, the Brazilian government's Action Plan for Prevention and Control of the Legal Amazon Deforestation was created in 2004 and the number of protected areas has increased considerably (Aragão et al., 2018). Under these improvements to regional environmental governance, it is unlikely that deforestation will return to the very high rates experiences in the early 2000s. Nevertheless, our maximum deforestation scenario is useful to understand the implications of environmental governance on deforestation and fire, and the impacts on air quality and public health.

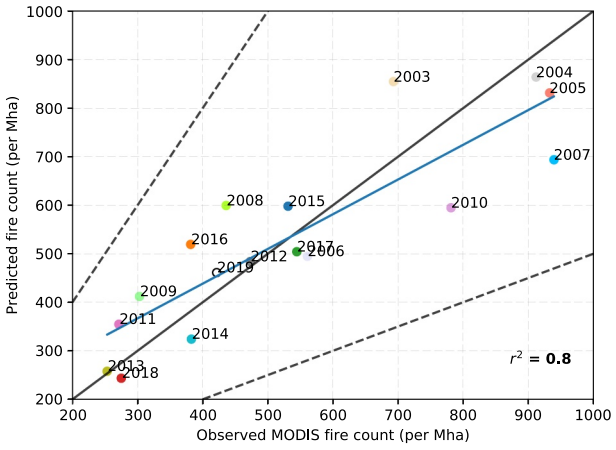

Figure 4. Observed versus predicted dry season active fire count (per Mha) for the Brazilian Legal Amazon (BLA). Lines represent linear regression (solid blue), 1:1 (solid black), and 1:2 (dashed black). BLA totals exclude the states of Roraima and Amapa (see Methods).

3.3. Impacts Fires on Air Quality and Public Health in 2019

We used a regional chemistry-climate model (WRF-Chem) to simulate the impacts of the fires in 2019 on air quality across the BLA. Dry season $PM_{2.5}$ concentrations >45 μg m^{-3} are simulated in southern and western BLA (Figure S12), matching the locations of deforestation and fire (Butt et al., 2020). Vegetation fires contribute up to 95% of $PM_{2.5}$ concentrations across the BLA, as well as contributing up to 40% of concentrations downwind of fires across Bolivia, Peru, and Brazil.

Air Quality Guidelines from the World Health Organization suggest 24-h mean $PM_{2.5}$ concentrations should not exceed 25 μg m^{-3} (WHO, 2006). Populations across large regions of South America are exposed to greater $PM_{2.5}$ concentrations during the dry season, with negative implications for public health. We combined simulated $PM_{2.5}$ concentrations with exposure-response relationships to estimate the public health impacts of exposure to fire-derived $PM_{2.5}$. Across our South American domain (Figure S4), we estimate that the prevention of all fires in the BLA would have avoided

Table 3
GLM Predicted Changes in Total Dry Season Fire Count in Year 2019 Based on Minimum and Maximum Deforestation Rate for the Period 2003 to 2019 are Also Shown

State	Deforestation rate 2019 (km^2)	Deforestation rate maximum km^2 (year)	Deforestation rate minimum km^2 (year)	Change in predicted 2019 fires with maximum deforestation (%)	Change in predicted 2019 fires with minimum deforestation (%)
Acre	688	1,078 (2003)	167 (2015)	+69.	−93.
Amazonas	1,421	1,558 (2003)	405 (2009)	+5	−41.
Maranhão	215	1,271 (2008)	209 (2015)	+63.	−0.4
Mato Grosso	1,685	11,814 (2004)	757 (2012)	+137.	−12
Para	3,862	8,870 (2004)	1,741 (2012)	+112.	−47.
Rondônia	1,245	3,858 (2004)	435 (2010)	+160.	−50.
Tocantins	21	271 (2005)	21 (2019)	+18.	0

Note. No changes in fires are predicted for Tocantins under the minimum deforestation scenario because deforestation in 2019 was the lowest observed between 2003 and 2019 in that state.
Abbreviation: GLM, general linear modeling.

367,429 (95th Uncertainty Interval [95UI] 316,253–425,285) DALYs and 9,469 (95UI: 9,162–9,776) premature deaths in 2019 (Table S3, Figure S13). Our estimate agrees with previous studies which estimated public health benefits of preventing South American fires to be 5,000–16,800 avoidable deaths per year (Butt et al., 2020; Johnston et al., 2012; Nawaz & Henze, 2020; Reddington et al., 2015). Previous studies use different exposure-response relationships and analyzed different domains, driving much of the difference in estimates. We used the GEMM exposure-response model (Burnett et al., 2018), which is consistent with the latest exposure-outcome associations for ambient $PM_{2.5}$, and to be conservative of risk estimates at higher exposures. In our study, fires within the BLA accounts for 37% of the South American domain avoided DALYs and 52% of avoided deaths, and so benefits greatly from fire prevention. States in the BLA experience substantial per-capita public health benefits, with large avoided DALYs rates (>900 per 100,000 people) and death rates (>20 per 100,000 people) (Table S3, Figure S13), under a scenario of no fire.

3.4. Impact of Increased Deforestation on Air Quality and Public Health

Previous estimates using scenarios of complete fire prevention are unrealistic: not all fires are caused by humans and it would not be possible to prevent all fires. We used our different deforestation scenarios to estimate the impacts of increased deforestation on fire count, pollutant emissions (Figure S14), air quality, and public health. We used WRF-Chem along with our predictions of fire count to simulate the change in air pollution under low and high deforestation scenarios (Figure 5). These deforestation scenarios span the range that has been observed over the last 2 decades. If deforestation had been reduced to the minimum experienced during 2003–2019, $PM_{2.5}$ concentrations in 2019 would have been reduced by up to 50%, whereas under the maximum they would have increased by up to 130%. Therefore our anal-

Table 4
Domain Wide Health Burden in 2019 (Baseline) and the Absolute Change in Health Burden Under the Minimum and Maximum Deforestation Scenarios Relative to the Baseline

Scenario	DALYs	Mortality
2019 (baseline)	367,429 (316,253–425,285)	9,469 (9,162–9,776)
Minimum	−132,200 (95UI: 113,100–153,700)	−3,400 (95UI: 3,300–3,550)
Maximum	+305,700 (95UI: 262,700–354,200)	+7,900 (95UI: 7,600–8,200)

Abbreviation: DALYs, disability-adjusted life years.

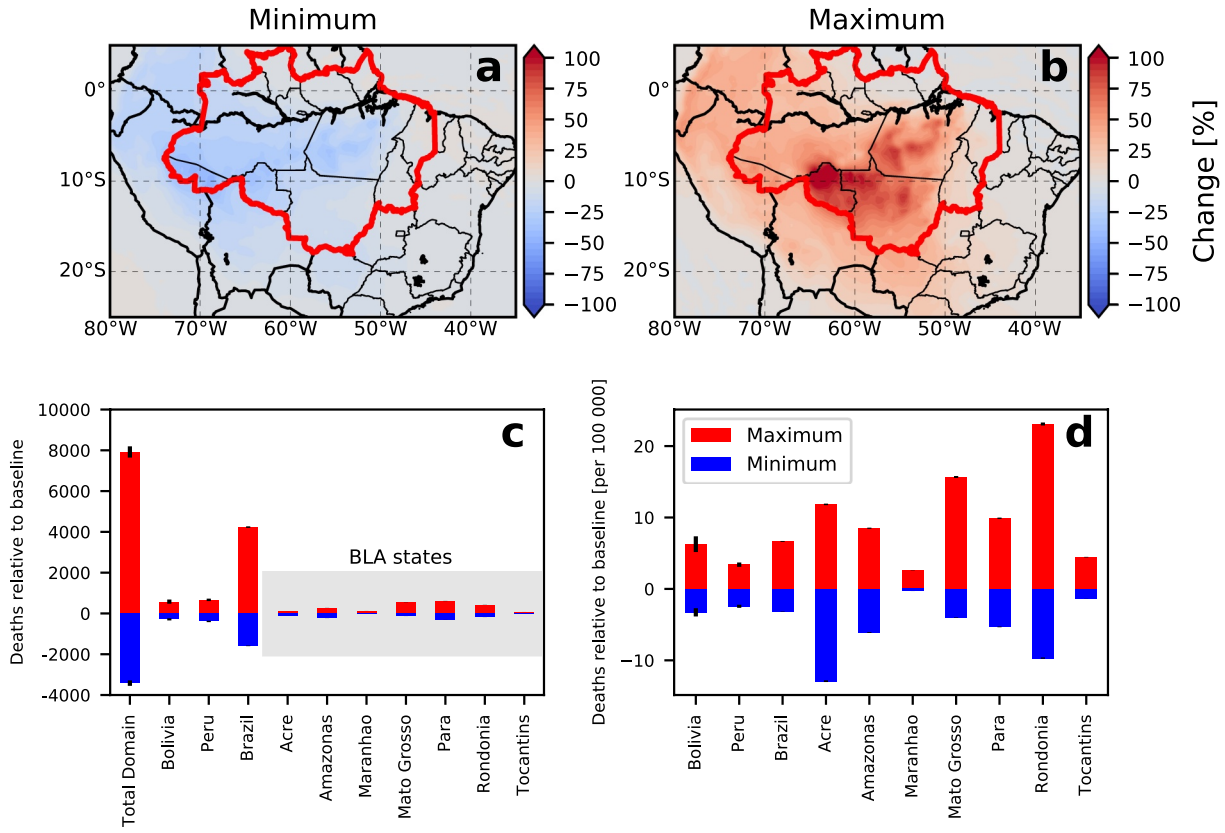

Figure 5. Impacts of deforestation on air quality and public health. Percentage change in dry season mean surface PM2.5 concentrations in 2019 under (a) minimum and (b) maximum deforestation scenario relative to the baseline. Health burden under maximum (red) and minimum (blue) deforestation scenarios relative to the baseline showing (c) total premature deaths, and (d) death rate per 100,000 people. Total Domain burden in (c) is deaths summed across our modeling domain (Figure 4), while the gray box highlights Brazilian Legal Amazon states analyzed in this study.

ysis shows that air quality in 2019 would have been better had deforestation levels been reduced to the minimum observed during 2003–2019, but also could have been much worse had deforestation levels been at the maximum experienced over this period. We then estimated the impacts of air pollution under these scenarios on public health (Figures 5c and 5d and Figure S15). Improved air quality under the minimum deforestation scenario would have resulted in 132,200 (95UI: 113,100–153,700) fewer DALYs and 3,400 (95UI: 3,300–3,550) fewer premature deaths (Table 4). This means that the increase in deforestation between 2014 and 2019 increased the disease burden by 56% in 2019. In contrast, if deforestation had increased to the maximum experienced during 2003–2019, the total avoidable burden of disease would have increased by nearly a further factor of 2, resulting in an additional 305,700 (95UI: 262,700–354,200) DALYs and 7,900 (95UI: 7,600–8,200) premature deaths (Table 4). States in the BLA with considerable deforestation and fire, experienced the greatest reductions in per-capita disease burden under the low deforestation scenario (Figure 5d), and greatest increases in disease burden under high deforestation rates.

Studies aiming to understand how fire regimes will change in the future highlight the strong climatic control on future forest flammability (Brando et al., 2020; Le Page et al., 2017). Our analysis confirms that in addition to climate, deforestation rate has a strong control on the incidence of fire (Aragão et al., 2008, 2018). We show that increased rates of deforestation between 2014 and 2019 has caused increased fire count, degrading air quality with substantial public health impacts. Efforts to reduce fire must focus on reducing the deforestation rate, in addition to fire management and suppression. Despite recent increases, deforestation rates across the BLA are still less than the high levels experienced before 2014. We demonstrate strong benefits of improved environmental governance on air quality and public health across the Amazon.

Conflict of Interest

The authors declare no conflicts of interest relevant to this study.

Data Availability Statement

The data that support the findings of this study are available at https://doi.org/10.5518/1017

Acknowledgments
This work received funding from the European Research Council (ERC) under the European Union's Horizon 2020 research and innovation programme (Grant agreement no. 771492) and the Natural Environmental Research Council (NE/J009822/1). Dominick V. Spracklen acknowledges a Philip Leverhulme Award. This work was undertaken on Advanced Research Computing, part of the High Performance Computing facilities at the University of Leeds, UK.

References

Alencar, A. A., Brando, P. M., Asner, G. P., & Putz, F. E. (2015). Landscape fragmentation, severe drought, and the new Amazon forest fire regime. *Ecological Applications*, *25*(6), 1493–1505. https://doi.org/10.1890/14-1528.1

Anderson, L. O., Aragão, L. E. O. C., Gloor, M., Arai, E., Adami, M., Saatchi, S. S., et al. (2015). Disentangling the contribution of multiple land covers to fire-mediated carbon emissions in Amazonia during the 2010 drought. *Global Biogeochemical Cycles*, *29*(10), 1739–1753. https://doi.org/10.1002/2014gb005008

Aragão, L. E. O. C., Anderson, L. O., Fonseca, M. G., Rosan, T. M., Vedovato, L. B., Wagner, F. H., et al. (2018). 21st Century drought-related fires counteract the decline of Amazon deforestation carbon emissions. *Nature Communications*, *9*(1), 1–12. https://doi.org/10.1038/s41467-017-02771-y

Aragão, L. E. O. C., Malhi, Y., Barbier, N., Lima, A., Shimabukuro, Y., Anderson, L., & Saatchi, S. (2008). Interactions between rainfall, deforestation and fires during recent years in the Brazilian Amazonia. *Philosophical Transactions of the Royal Society B: Biological Sciences*, *363*(1498), 1779–1785. https://doi.org/10.1098/rstb.2007.0026

Aragão, L. E. O. C., Malhi, Y., Roman-Cuesta, R. M., Saatchi, S., Anderson, L. O., & Shimabukuro, Y. E. (2007). Spatial patterns and fire response of recent Amazonian droughts. *Geophysical Research Letters*, *34*(7). https://doi.org/10.1029/2006gl028946

Aragão, L. E. O. C., Poulter, B., Barlow, J. B., Anderson, L. O., Malhi, Y., Saatchi, S., et al. (2014). Environmental change and the carbon balance of Amazonian forests. *Biological Reviews*, *89*(4), 913–931. https://doi.org/10.1111/brv.12088

Archer-Nicholls, S., Lowe, D., Darbyshire, E., Morgan, W. T., Bela, M. M., Pereira, G., et al. (2015). Characterising Brazilian biomass burning emissions using WRF-Chem with MOSAIC sectional aerosol. *Geoscientific Model Development*, *8*(3), 549–577. https://doi.org/10.5194/gmd-8-549-2015

Archer-Nicholls, S., Lowe, D., Schultz, D. M., & McFiggans, G. (2016). Aerosol–radiation–cloud interactions in a regional coupled model: The effects of convective parameterisation and resolution. *Atmospheric Chemistry and Physics*, *16*(9), 5573. https://doi.org/10.5194/acp-16-5573-2016

Artaxo, P., Rizzo, L. V., Brito, J. F., Barbosa, H. M. J., Arana, A., Sena, E. T., et al. (2013). Atmospheric aerosols in Amazonia and land use change: From natural biogenic to biomass burning conditions. *Faraday Discussions*, *165*, 203–235. https://doi.org/10.1039/c3fd00052d

Assis, F., Ferreira, K. R., Vinhas, L., Maurano, L., Almeida, C., Carvalho, A., et al. (2019). TerraBrasilis: A Spatial Data Analytics Infrastructure for Large-Scale Thematic Mapping. *ISPRS International Journal of Geo-Information*, *8*(11). https://doi.org/10.3390/ijgi8110513

Baker, J., & Spracklen, D. (2019). Climate benefits of intact Amazon forests and the biophysical consequences of disturbance. *Frontiers in Forests and Global Change*, *2*, 47. https://doi.org/10.3389/ffgc.2019.00047

Barlow, J., Berenguer, E., Carmenta, R., & França, F. (2019). Clarifying Amazonia's burning crisis. *Global Change Biology*. https://doi.org/10.1111/gcb.14872

Barlow, J., Lennox, G. D., Ferreira, J., Berenguer, E., Lees, A. C., Nally, R. M., et al. (2016). Anthropogenic disturbance in tropical forests can double biodiversity loss from deforestation. *Nature*, *535*(7610), 144–147. https://doi.org/10.1038/nature18326

Barlow, J., Peres, C. A., Lagan, B. O., & Haugaasen, T. (2003). Large tree mortality and the decline of forest biomass following Amazonian wildfires. *Ecology Letters*, *6*(1), 6–8.

Brando, P. M., Balch, J. K., Nepstad, D. C., Morton, D. C., Putz, F. E., Coe, M. T., et al. (2014). Abrupt increases in Amazonian tree mortality due to drought–fire interactions. *Proceedings of the National Academy of Sciences of the United States of America*, *111*(17), 6347–6352. https://doi.org/10.1073/pnas.1305499111

Brando, P. M., Soares-Filho, B., Rodrigues, L., Assunção, A., Morton, D., Tuchschneider, D., et al. (2020). The gathering firestorm in southern Amazonia. *Science advances*, *6*(2), eaay1632. https://doi.org/10.1126/sciadv.aay1632

Brito, J., Rizzo, L. V., Morgan, W. T., Coe, H., Johnson, B., Haywood, J., et al. (2014). Ground-based aerosol characterization during the South American Biomass Burning Analysis (SAMBBA) field experiment. *Atmospheric Chemistry and Physics*, *14*(22), 12069–12083. https://doi.org/10.5194/acp-14-12069-2014

Burnett, R. T., Chen, H., Szyszkowicz, M., Fann, N., Hubbell, B., Arden Pope, C., III, et al. (2018). Global estimates of mortality associated with long-term exposure to outdoor fine particulate matter. *Proceedings of the National Academy of Sciences of the United States of America*, *115*(38), 9592–9597.

Burnett, R. T., Pope, C. A., Ezzati, M., Olives, C., Lim, S. S., Mehta, S., et al. (2014). An integrated risk function for estimating the global burden of disease attributable to ambient fine particulate matter exposure. *Environmental Health Perspectives*, *122*(4), 397–403. https://doi.org/10.1289/ehp.1307049

Butt, E. W., Conibear, L., Reddington, C. L., Darbyshire, E., Morgan, W. T., Coe, H., et al. (2020). Large air quality and human health impacts due to Amazon forest and vegetation fires. *Environmental Research Communications*, *2*(9), 095001. https://doi.org/10.1088/2515-7620/abb0db

Cano-Crespo, A., Oliveira, P. J. C., Boit, A., Cardoso, M., & Thonicke, K. (2015). Forest edge burning in the Brazilian Amazon promoted by escaping fires from managed pastures. *Journal of Geophysical Research: Biogeosciences*, *120*(10), 2095–2107.

Center for International Earth Science Information Network—CIESIN—Columbia University. (2018). *Gridded population of the World, version 4 (GPWv4): Population count, revision 11*. NASA Socioeconomic Data and Applications Center (SEDAC). https://doi.org/10.7927/H4JW8BX5

Chen, Y., Morton, D. C., Jin, Y., Collatz, G. J., Kasibhatla, P. S., van der Werf, G. R., et al. (2013). Long-term trends and interannual variability of forest, savanna and agricultural fires in South America. *Carbon Management*, *4*(6), 617–638. https://doi.org/10.4155/cmt.13.61

Chen, Y., Randerson, J. T., Morton, D. C., DeFries, R. S., Collatz, G. J., Kasibhatla, P. S., et al. (2011). Forecasting fire season severity in South America using sea surface temperature anomalies. *Science*, *334*(6057), 787–791. https://doi.org/10.1126/science.1209472

Chin, M., Rood, R. B., Lin, S.-J., Müller, J.-F., & Thompson, A. M. (2000). Atmospheric sulfur cycle simulated in the global model GOCART: Model description and global properties. *Journal of Geophysical Research*, *105*(D20), 24671–24687. https://doi.org/10.1029/2000jd900384
Cochrane, M. A. (2003). Fire science for rainforests. *Nature*, *421*(6926), 913–919. https://doi.org/10.1038/nature01437
Cochrane, M. A., Alencar, A., Schulze, M. D., Souza, C. M., Jr., Nepstad, D. C., Lefebvre, P., & Davidson, E. A. (1999). Positive feedbacks in the fire dynamic of closed canopy tropical forests. *Science*, *284*(5421), 1832–1835. https://doi.org/10.1126/science.284.5421.1832
Cohen, A. J., Brauer, M., Burnett, R., Anderson, H. R., Frostad, J., Estep, K., et al. (2017). Estimates and 25-year trends of the global burden of disease attributable to ambient air pollution: An analysis of data from the Global Burden of Diseases Study 2015. *The Lancet*, *389*(10082), 1907–1918. https://doi.org/10.1016/s0140-6736(17)30505-6
Conibear, L., Butt, E. W., Knote, C., Arnold, S. R., & Spracklen, D. V. (2018). Residential energy use emissions dominate health impacts from exposure to ambient particulate matter in India. *Nature Communications*, *9*(1), 1–9. https://doi.org/10.1038/s41467-018-02986-7
Crippa, P., Castruccio, S., Archer-Nicholls, S., Lebron, G. B., Kuwata, M., Thota, A., et al. (2016). Population exposure to hazardous air quality due to the 2015 fires in Equatorial Asia. *Scientific Reports*, *6*, 37074. https://doi.org/10.1038/srep37074
ECMWF. (2017). *Copernicus Climate Change Service (C3S): ERA5: Fifth generation of ECMWF atmospheric reanalyzes of the global climate*. Copernicus Climate Change Service Climate Data Store (CDS).
Emmons, L. K., Walters, S., Hess, P. G., Lamarque, J. F., Pfister, G. G., Fillmore, D., et al. (2010). *Description and evaluation of the model for ozone and related chemical tracers, version 4 (MOZART-4)*.
Fernandes, K., Baethgen, W., Bernardes, S., DeFries, R., DeWitt, D. G., Goddard, L., et al. (2011). North Tropical Atlantic influence on western Amazon fire season variability. *Geophysical Research Letters*, *38*(12). https://doi.org/10.1029/2011gl047392
Funk, C. C., Peterson, P. J., Landsfeld, M. F., Pedreros, D. H., Verdin, J. P., Rowland, J. D., et al. (2014). *A quasi-global precipitation time series for drought monitoring* (US Geological Survey data series 832, p. 4). https://doi.org/10.3133/ds832
Giglio, L. (2007). Characterization of the tropical diurnal fire cycle using VIRS and MODIS observations. *Remote Sensing of Environment*, *108*(4), 407–421. https://doi.org/10.1016/j.rse.2006.11.018
Giglio, L., Csiszar, I., & Justice, C. O. (2006). Global distribution and seasonality of active fires as observed with the Terra and Aqua Moderate Resolution Imaging Spectroradiometer (MODIS) sensors. *Journal of Geophysical Research*, *111*(G2). https://doi.org/10.1029/2005jg000142
Giglio, L., Descloitres, J., Justice, C. O., & Kaufman, Y. J. (2003). An enhanced contextual fire detection algorithm for MODIS. *Remote Sensing of Environment*, *87*(2–3), 273–282. https://doi.org/10.1016/s0034-4257(03)00184-6
Giglio, L., Randerson, J. T., & van der Werf, G. R. (2013). Analysis of daily, monthly, and annual burned area using the fourth-generation global fire emissions database (GFED4). *Journal of Geophysical Research: Biogeosciences*, *118*(1), 317–328. https://doi.org/10.1002/jgrg.20042
Grell, G. A., & Dévényi, D. (2002). A generalized approach to parameterizing convection combining ensemble and data assimilation techniques. *Geophysical Research Letters*, *29*(14). https://doi.org/10.1029/2002gl015311
Grell, G. A., Peckham, S. E., Schmitz, R., McKeen, S. A., Frost, G., Skamarock, W. C., & Eder, B. (2005). Fully coupled "online" chemistry within the WRF model. *Atmospheric Environment*, *39*(37), 6957–6975. https://doi.org/10.1016/j.atmosenv.2005.04.027
Guenther, A., Karl, T., Harley, P., Wiedinmyer, C., Palmer, P. I., & Geron, C. (2006). Estimates of global terrestrial isoprene emissions using MEGAN (Model of Emissions of Gases and Aerosols from Nature). *Atmospheric Chemistry and Physics*, *6*(11), 3181–3210. https://doi.org/10.5194/acp-6-3181-2006
Hansen, M. C., Potapov, P. V., Moore, R., Hancher, M., Turubanova, S. A., Tyukavina, A., et al. (2013). High-resolution global maps of 21st-century forest cover change. *Science*, *342*(6160), 850–853. https://doi.org/10.1126/science.1244693
Hijmans, R. (2012). *Global administrative areas (boundaries)*. Museum of Vertebrate Zoology and the International Rice Research Institute, University of California.
Hodzic, A., & Knote, C. (2014). WRF-Chem 3.6.1: MOZART gas-phase chemistry with MOSAIC aerosols (Vol. 7). Atmospheric Chemistry Division (ACD), National Center for Atmospheric Research (NCAR).
Janssens-Maenhout, G., Crippa, M., Guizzardi, D., Dentener, F., Muntean, M., Pouliot, G., et al. (2015). HTAP_v2.2: A mosaic of regional and global emission grid maps for 2008 and 2010 to study hemispheric transport of air pollution. *Atmospheric Chemistry and Physics*, *15*(19), 11411–11432. https://doi.org/10.5194/acp-15-11411-2015
Johnston, F. H., Henderson, S. B., Chen, Y., Randerson, J. T., Marlier, M., DeFries, R. S., et al. (2012). Estimated global mortality attributable to smoke from landscape fires. *Environmental Health Perspectives*, *120*(5), 695–701. https://doi.org/10.1289/ehp.1104422
Kiely, L., Spracklen, D. V., Wiedinmyer, C., Conibear, L., Reddington, C. L., Arnold, S. R., et al. (2020). Air quality and health impacts of vegetation and peat fires in Equatorial Asia during 2004–2015. *Environmental Research Letters*, *15*(9), 094054. https://doi.org/10.1088/1748-9326/ab9a6c
Knote, C., Hodzic, A., & Jimenez, J. L. (2015). The effect of dry and wet deposition of condensable vapors on secondary organic aerosols concentrations over the continental US. *Atmospheric Chemistry and Physics*, *15*(1), 1–18. https://doi.org/10.5194/acp-15-1-2015
Knote, C., Hodzic, A., Jimenez, J. L., Volkamer, R., Orlando, J. J., Baidar, S., et al. (2014). Simulation of semi-explicit mechanisms of SOA formation from glyoxal in aerosol in a 3-D model. *Atmospheric Chemistry and Physics*, *14*(12), 6213–6239. https://doi.org/10.5194/acp-14-6213-2014
Kodros, J. K., Wiedinmyer, C., Ford, B., Cucinotta, R., Gan, R., Magzamen, S., & Pierce, J. R. (2016). Global burden of mortalities due to chronic exposure to ambient PM2. 5 from open combustion of domestic waste. *Environmental Research Letters*, *11*(12), 124022. https://doi.org/10.1088/1748-9326/11/12/124022
Kolusu, S., Marsham, J. H., Mulcahy, J., Johnson, B., Dunning, C., Bush, M., & Spracklen, D. V. (2015). Impacts of Amazonia biomass burning aerosols assessed from short-range weather forecasts. *Atmospheric Chemistry and Physics*, *15*(21), 12251–12266. https://doi.org/10.5194/acp-15-12251-2015
Koplitz, S. N., Mickley, L. J., Marlier, M. E., Buonocore, J. J., Kim, P. S., Liu, T., et al. (2016). Public health impacts of the severe haze in Equatorial Asia in September–October 2015: Demonstration of a new framework for informing fire management strategies to reduce downwind smoke exposure. *Environmental Research Letters*, *11*(9), 094023. https://doi.org/10.1088/1748-9326/11/9/094023
Lelieveld, J., Evans, J. S., Fnais, M., Giannadaki, D., & Pozzer, A. (2015). The contribution of outdoor air pollution sources to premature mortality on a global scale. *Nature*, *525*(7569), 367. https://doi.org/10.1038/nature15371
Le Page, Y., Morton, D., Hartin, C., Bond-Lamberty, B., Pereira, J. M. C., Hurtt, G., & Asrar, G. (2017). Synergy between land use and climate change increases future fire risk in Amazon forests. *Earth System Dynamics*, *8*, 1237–1246. https://doi.org/10.5194/esd-8-1237-2017
Levy, R., Mattoo, S., Munchak, L. A., Remer, L. A., Sayer, A. M., Patadia, F., & Hsu, N. C. (2013). The Collection 6 MODIS aerosol products over land and ocean. *Atmospheric Measurement Techniques*, *6*(11), 2989. https://doi.org/10.5194/amt-6-2989-2013

Libonati, R., Pereira, J. M. C., Da Camara, C. C., Peres, L. F., Oom, D., Rodrigues, J. A., et al. (2021). Twenty-first century droughts have not increasingly exacerbated fire season severity in the Brazilian Amazon. *Scientific Reports*, *11*(1), 1–13. https://doi.org/10.1038/s41598-021-82158-8

Lima, C. H., AghaKouchak, A., & Randerson, J. T. (2018). Unraveling the role of temperature and rainfall on active fires in the Brazilian Amazon using a nonlinear Poisson model. *Journal of Geophysical Research: Biogeosciences*, *123*(1), 117–128. https://doi.org/10.1002/2017jg003836

Lipsett, M. J., Ostro, B. D., Reynolds, P., Goldberg, D., Hertz, A., Jerrett, M., et al. (2011). Long-term exposure to air pollution and cardiorespiratory disease in the California teachers study cohort. *American Journal of Respiratory and Critical Care Medicine*, *184*(7), 828–835. https://doi.org/10.1164/rccm.201012-2082oc

Liu, L., Cheng, Y., Wang, S., Wei, C., Pöhlker, M. L., Pöhlker, C., et al. (2020). Impact of biomass burning aerosols on radiation, clouds, and precipitation over the Amazon during the dry season: Dependence of aerosol-cloud and aerosol-radiation interactions on aerosol loading. *Atmospheric Chemistry and Physics Discussions*.

Lovejoy, T. E., & Nobre, C. (2018). *Amazon tipping point*. American Association for the Advancement of Science. https://doi.org/10.1126/sciadv.aat2340

Marenco, F., Johnson, B., Langridge, J. M., Mulcahy, J., Benedetti, A., Remy, S., et al. (2016). *On the vertical distribution of smoke in the Amazonian atmosphere during the dry season*.

Marengo, J. A., & Espinoza, J. C. (2016). Extreme seasonal droughts and floods in Amazonia: Causes, trends and impacts. *International Journal of Climatology*, *36*(3), 1033–1050. https://doi.org/10.1002/joc.4420

Martin, S. T., Andreae, M. O., Artaxo, P., Baumgardner, K., Chen, Q., Goldstein, A. H., et al. (2010). Sources and properties of Amazonian aerosol particles. *Reviews of Geophysics*, *48*(2). https://doi.org/10.1029/2008RG000280

Miller, K. A., Siscovick, D. S., Sheppard, L., Shepherd, K., Sullivan, J. H., Anderson, G. L., & Kaufman, J. D. (2007). Long-term exposure to air pollution and incidence of cardiovascular events in women. *New England Journal of Medicine*, *356*(5), 447–458. https://doi.org/10.1056/nejmoa054409

Mishra, A. K., Lehahn, Y., Rudich, Y., & Koren, I. (2015). Co-variability of smoke and fire in the Amazon basin. *Atmospheric Environment*, *109*, 97–104. https://doi.org/10.1016/j.atmosenv.2015.03.007

Morrison, H., Thompson, G., & Tatarskii, V. (2009). Impact of cloud microphysics on the development of trailing stratiform precipitation in a simulated squall line: Comparison of one-and two-moment schemes. *Monthly Weather Review*, *137*(3), 991–1007. https://doi.org/10.1175/2008mwr2556.1

Morton, D., Defries, R. S., Randerson, J. T., Giglio, L., Schroeder, W., & Van Der Werf, G. R. (2008). Agricultural intensification increases deforestation fire activity in Amazonia. *Global Change Biology*, *14*(10), 2262–2275. https://doi.org/10.1111/j.1365-2486.2008.01652.x

National Center for Atmospheric Research. (2019). *ACOM MOZART-4/GEOS-5 global model output*. Retrieved from http://www.acom.ucar.edu/wrf-chem/mozart.shtml

Nawaz, M., & Henze, D. (2020). Premature deaths in Brazil associated with long-term exposure to PM2.5 from Amazon fires between 2016-2019. *GeoHealth*, *4*. https://doi.org/10.1029/2020GH000268

Nepstad, D. C., Stickler, C. M., Filho, B. S., & Merry, F. (2008). Interactions among Amazon land use, forests and climate: Prospects for a near-term forest tipping point. *Philosophical Transactions of the Royal Society B: Biological Sciences*, *363*(1498), 1737–1746. https://doi.org/10.1098/rstb.2007.0036

Olivier, J., Peters, J., Granier, C., Petron, G., Muller, J. F., & Wallens, S. (2003). *Present and future surface emissions of atmospheric compounds* (POET report #2, EU project EVK2-1999-00011).

Puett, R. C., Hart, J. E., Yanosky, J. D., Paciorek, C., Schwartz, J., Suh, H., et al. (2009). Chronic fine and coarse particulate exposure, mortality, and coronary heart disease in the Nurses' Health Study. *Environmental Health Perspectives*, *117*(11), 1697–1701. https://doi.org/10.1289/ehp.0900572

Ray, D., Nepstad, D., & Moutinho, P. (2005). Micrometeorological and canopy controls of fire susceptibility in a forested Amazon landscape. *Ecological Applications*, *15*(5), 1664–1678. https://doi.org/10.1890/05-0404

Reddington, C. L., Butt, E. W., Ridley, D. A., Artaxo, P., Morgan, W. T., Coe, H., et al. (2015). Air quality and human health improvements from reductions in deforestation-related fire in Brazil. *Nature Geoscience*, *8*(10), 768. https://doi.org/10.1038/ngeo2535

Reddington, C. L., Morgan, W. T., Darbyshire, E., Brito, J., Coe, H., Artaxo, P., et al. (2019). Biomass burning aerosol over the Amazon: Analysis of aircraft, surface and satellite observations using a global aerosol model. *Atmospheric Chemistry and Physics*, *19*(14), 9125–9152. https://doi.org/10.5194/acp-19-9125-2019

Reddington, C. L., Spracklen, D. V., Artaxo, P., Ridley, D. A., Rizzo, L. V., & Arana, A. (2016). Analysis of particulate emissions from tropical biomass burning using a global aerosol model and long-term surface observations. *Atmospheric Chemistry and Physics*, *16*(17), 11083–11106. https://doi.org/10.5194/acp-16-11083-2016

Roth, G. A., Abate, D., Abate, K. H., Abay, S. M., Abbafati, C., Abbasi, N., et al. (2018). Global, regional, and national age-sex-specific mortality for 282 causes of death in 195 countries and territories, 1980–2017: A systematic analysis for the Global Burden of Disease Study 2017. *The Lancet*, *392*(10159), 1736–1788.

Sant'Anna, A. A., Rocha, R., & Amazônia (IPAM) and Human Rights Watch. (2020). *Health impacts of deforestation-related fires in the Brazilian Amazon*. Instituto de Estudos para Políticas de Saúde (IEPS) to the joint report by IEPS, the Instituto.

Silvestrini, R. A., Soares-Filho, B. S., Nepstad, D., Coe, M., Rodrigues, H., & Assunção, R. (2011). Simulating fire regimes in the Amazon in response to climate change and deforestation. *Ecological Applications*, *21*(5), 1573–1590. https://doi.org/10.1890/10-0827.1

Spracklen, D. V., Arnold, S. R., & Taylor, C. M. (2012). Observations of increased tropical rainfall preceded by air passage over forests. *Nature*, *489*(7415), 282–285. https://doi.org/10.1038/nature11390

Spracklen, D. V., & Garcia-Carreras, L. (2015). The impact of Amazonian deforestation on Amazon basin rainfall. *Geophysical Research Letters*, *42*(21), 9546–9552. https://doi.org/10.1002/2015gl066063

vanMarle, M. J., Field, R. D., van der Werf, G. R., Estrada de Wagt, I. A., Houghton, R. A., Rizzo, L. V., et al. (2017). Fire and deforestation dynamics in Amazonia (1973–2014). *Global Biogeochemical Cycles*, *31*(1), 24–38. https://doi.org/10.1002/2016gb005445

Wan, Z., Hook, S., & Hulley, G. (2015). *MOD11C3 MODIS/Terra land surface temperature/emissivity monthly L3 global 0.05Deg CMG V006*. NASA EOSDIS Land Processes DAAC.

WHO. (2006). *World Health Organization air quality guidelines for particulate matter, ozone, nitrogen dioxide and sulfur dioxide: Global update 2005: Summary of risk assessment*. World Health Organization.

Wiedinmyer, C., Akagi, S. K., Yokelson, R. J., Emmons, L. K., Al-Saadi, J. A., Orlando, J. J., et al. (2011). The Fire INventory from NCAR (FINN): A high resolution global model to estimate the emissions from open burning. *Geoscientific Model Development*, *4*(3), 625. https://doi.org/10.5194/gmd-4-625-2011

Withey, K., Berenguer, E., Palmeira, A. F., Espírito-Santo, F. D. B., Lennox, G. D., Silva, C. V. J., et al. (2018). Quantifying immediate carbon emissions from El Niño-mediated wildfires in humid tropical forests. *Philosophical Transactions of the Royal Society B: Biological Sciences*, *373*(1760), 20170312. https://doi.org/10.1098/rstb.2017.0312

Zaveri, R. A., Easter, R. C., Fast, J. D., & Peters, L. K. (2008). Model for simulating aerosol interactions and chemistry (MOSAIC). *Journal of Geophysical Research*, *113*(D13). https://doi.org/10.1029/2007jd008782

Zemp, D. C., Schleussner, C. F., Barbosa, H. M. J., Hirota, M., Montade, V., Sampaio, G., et al. (2017). Self-amplified Amazon forest loss due to vegetation-atmosphere feedbacks. *Nature Communications*, *8*(1), 1–10. https://doi.org/10.1038/ncomms14681